JVI Journals.ASM.org

Plasticity and Virus Specificity of the Airway Epithelial Cell Immune Response during Respiratory Virus Infection

Ioannis Ioannidis,[a] Beth McNally,[a] Meredith Willette,[a] Mark E. Peeples,[a,b] Damien Chaussabel,[c] Joan E. Durbin,[d] Octavio Ramilo,[a,b] Asuncion Mejias,[a,b] and Emilio Flaño[a,b]

Center for Vaccines and Immunity, The Research Institute at Nationwide Children's Hospital, Columbus, Ohio, USA[a]; Department of Pediatrics, The Ohio State University College of Medicine, Columbus, Ohio, USA[b]; Benaroya Research Institute, Seattle, Washington, USA[c]; and Department of Pathology, New York University, New York, New York, USA[d]

Airway epithelial cells (AECs) provide the first line of defense in the respiratory tract and are the main target of respiratory viruses. Here, using oligonucleotide and protein arrays, we analyze the infection of primary polarized human AEC cultures with influenza virus and respiratory syncytial virus (RSV), and we show that the immune response of AECs is quantitatively and qualitatively virus specific. Differentially expressed genes (DEGs) specifically induced by influenza virus and not by RSV included those encoding interferon B1 (IFN-B1), type III interferons (interleukin 28A [IL-28A], IL-28B, and IL-29), interleukins (IL-6, IL-1A, IL-1B, IL-23A, IL-17C, and IL-32), and chemokines (CCL2, CCL8, and CXCL5). Lack of type I interferon or STAT1 signaling decreased the expression and secretion of cytokines and chemokines by the airway epithelium. We also observed strong basolateral polarization of the secretion of cytokines and chemokines by human and murine AECs during infection. Importantly, the antiviral response of human AECs to influenza virus or to RSV correlated with the infection signature obtained from peripheral blood mononuclear cells (PBMCs) isolated from patients with acute influenza or RSV bronchiolitis, respectively. IFI27 (also known as ISG12) was identified as a biomarker of respiratory virus infection in both AECs and PBMCs. In addition, the extent of the transcriptional perturbation in PBMCs correlated with the clinical disease severity. Our results demonstrate that the human airway epithelium mounts virus-specific immune responses that are likely to determine the subsequent systemic immune responses and suggest that the absence of epithelial immune mediators after RSV infection may contribute to explaining the inadequacy of systemic immunity to the virus.

Airway epithelial cells (AECs) represent the first barrier against inhaled microorganisms and actively prevent the entry of respiratory pathogens. The airway epithelium is a ciliated, pseudostratified, columnar epithelium consisting of ciliated cells, basal cells, and secretory goblet cells that, together with locally produced IgA, provide mechanisms for mucociliary clearance of inhaled microorganisms (19). In response to antigenic insults, AECs participate in host defense mechanisms by producing cytokines and chemokines, such as interleukin 6 (IL-6), IL-8, IL-1α, RANTES, MIP-1α, granulocyte-macrophage colony-stimulating factor (GM-CSF), and granulocyte colony-stimulating factor (G-CSF) (1, 8, 21, 26, 44, 47, 48). Regulation of the intensity and duration of inflammation in the airways is critical for maintaining respiratory function, and thus, epithelial cells also mediate a plethora of processes with the goal of limiting airway inflammation (22). While there is compelling evidence showing that AECs participate in local immune responses in the airways, it is unclear to what extent their response contributes to or can forecast the subsequent systemic immune response.

Influenza virus and respiratory syncytial virus (RSV) are two of the leading etiologies of acute respiratory disease (13), and the epithelium of the airways is their main target. AECs respond to infection by initiating a cytokine cascade that triggers inflammation and, together with AEC death, contributes to lung pathogenesis (34, 50). Studies in mice have highlighted the importance of epithelial type I and/or type III interferons in the response to both RSV and influenza virus (24, 25, 33, 54). Analysis of nasal washes from children with RSV infection or influenza revealed that more children with influenza produced interferon and that the amount of interferon produced was significantly greater in influenza virus-infected children than in children infected with RSV (16). NF-κB and beta interferon (IFN-β)/IRF3 are central regulators of the response of epithelial cells to both RSV and influenza virus (2, 5, 29, 56), and both viruses encode interferon inhibitors (10, 49, 53). Importantly, polarization and stratification of AECs determine barrier integrity and the response during infection (7, 30, 52) to the extent that viruses, such as human parainfluenza virus type 3, RSV, or strains of influenza virus, show tropism for ciliated epithelial cells (51, 59, 60).

Here, we have investigated how the airway epithelium responds to RSV and influenza virus infection and to what extent the mucosal response can be related to systemic immune responses and disease severity. Transcriptional profiling has served to improve our understanding of disease pathogenesis by defining pathogen- or disease-specific transcriptional signatures (6, 20), and gene expression patterns obtained from peripheral blood can help discriminate patients with distinct infections (3, 41, 58). The advantage of this approach is that thousands of molecules can be simultaneously measured and analyzed in an unbiased manner, and the application of biological knowledge systems to these data

Received 7 November 2011 **Accepted** 27 February 2012
Published ahead of print 7 March 2012
Address correspondence to Emilio Flaño, emilio.flano@nationwidechildrens.org, or Asuncion Mejias, asuncion.mejias@nationwidechildrens.org.
Supplemental material for this article may be found at http://jvi.asm.org.

doi:10.1128/JVI.06757-11

allows the comparison of responses in different anatomical compartments and to different pathogens. In this study, we used two respiratory viruses that replicate at the mucosal site of entry. We found that the response of the airway epithelium to influenza virus or RSV infection was quantitatively and qualitatively virus specific, although it presented a common type I interferon signature. There was a significant correlation between the common differentially expressed genes (DEGs) of AECs exposed to RSV or influenza virus and those of peripheral blood mononuclear cells (PBMCs) isolated from patients with acute RSV and influenza virus infection, respectively. Moreover, the extent of transcriptional perturbation in PBMCs induced by RSV bronchiolitis or acute influenza correlated with disease severity in each respective cohort of patients. Our results indicate that respiratory-virus-specific signatures of infection are conserved across different anatomical compartments and cell populations and that peripheral blood responses are a reflection of the response at the mucosal site of infection and of the clinical severity of the disease.

MATERIALS AND METHODS

Primary human airway epithelial cell (hAEC) cultures. Human airway tracheobronchial epithelial cells from non-cystic fibrosis patients were obtained from airway specimens resected at lung transplantation following Nationwide Children's Hospital Institutional Review Board-approved protocols. Epithelial cells were removed from the mainstream bronchi by protease digestion and plastic adherence and plated at a density of 300,000 per well on permeable Transwell-Col supports. Cultures were maintained under air-liquid interface (ALI) for 4 to 6 weeks to form well differentiated, polarized cultures that resemble the *in vivo* pseudostratified mucociliary epithelium, as previously described (38).

Primary mouse airway epithelial cell (mAEC) cultures. Wild-type (WT) BALB/c mice were purchased from Harlan Laboratories, while BALB/c IFN-α/β receptor$^{-/-}$ (IFNAR$^{-/-}$) mice and STAT1$^{-/-}$ mice were bred in-house. All animals were maintained in biosafety level 2 (BL2) containment under pathogen-free conditions. The Institutional Animal Care and Use Committee at the Research Institute at Nationwide Children's Hospital approved all the animal studies described in this work. Tracheal epithelial cell isolation and culture were performed as previously described (43, 57). Nonadherent cells were seeded onto 12-mm diameter, 0.4-μm pore size clear polyester membranes (Corning-Costar) previously coated with a collagen solution. After reaching confluence, the cells were incubated under ALI, and when the transepithelial resistance was >1,000 W/cm^2, the basolateral medium was replaced with fresh medium every other day. Cultures were routinely used for experimentation 10 to 14 days post-ALI incubation.

Patients. Children with a median age of 2.4 (range, 1.5 to 8.6) months hospitalized with acute RSV and influenza virus infections were offered study enrollment after microbiologic confirmation of the diagnosis. Blood samples were collected from them within 42 to 72 h of hospitalization. We excluded children with suspected or proven polymicrobial infections, with underlying chronic medical conditions (i.e., congenital heart disease or renal insufficiency), or with immunodeficiency or those who received systemic steroids or other immunomodulatory therapies. The RSV cohort consisted of 51 patients with a median age of 2 (range, 1.5 to 3.9) months, and the influenza virus cohort had 28 patients with a median age of 5.5 (range, 1.4 to 21) months. Control samples were obtained from healthy children undergoing elective surgical procedures or at outpatient clinic visits. To exclude viral coinfections, we performed nasopharyngeal viral cultures of all subjects. We recruited 10 control patients for the RSV cohort with a median age of 6.7 (range, 5 to 10) months and 12 control patients for the influenza virus cohort with a median age of 18.5 (range, 10.5 to 26) months. The Institutional Review Boards at the University of Texas Southwestern Medical Center and Baylor Institute for Immunology Research approved this study, and informed consent was obtained from legal guardians prior to any study-related procedure.

Disease severity score. To classify patients with acute RSV infection or influenza based on disease severity, we applied an adapted score for bronchiolitis at the time of sample collection (4, 40). This score included documentation of percutaneous O_2 saturation, respiratory rate, subcostal retractions, general appearance, and auscultation. Each parameter was ranked as mild (0 to 5), moderate (6 to 10), or severe (11 to 15)), with a maximum clinical score of 15.

Blood samples. Blood samples (3 to 6 ml) were collected in acid-citrate-dextrose tubes (BD Vacutainer) and delivered at room temperature for microarray processing. PBMCs were isolated within 6 h of sample collection by density gradient centrifugation using Ficoll-Hypaque and lysed in RLT reagent (Qiagen) with β-mercaptoethanol. Samples were run blind and in batches by the same laboratory team to ensure standardization of quality and handling. From 2 to 5 μg of total RNA, cDNA was generated as a template for single-round *in vitro* transcription with biotin-labeled nucleotides using Affymetrix cDNA Synthesis and In Vitro Transcription kits (Affymetrix Inc.). Biotinylated cDNA targets were then purified and hybridized to the Affymetrix HG-U133 plus 2.0 chip arrays according to the manufacturer's standard protocols. The arrays were scanned using a laser confocal scanner (Agilent). Raw signal intensity values were normalized to the mean intensity of all measurements per gene chip and scaled to a target intensity value of 500 using the MAS 5.0 global scaling method to adjust for possible chip-to-chip variations in hybridization intensities (GeneChip Operating System version 1.0).

Viruses. Influenza A/WSN/33 (H1N1) and influenza A/Udorn/72 (H3N2) viruses were grown for 48 to 72 h in day 10 embryonated chicken eggs at 37.5°C, and virus titers were determined by an immunofluorescence focus assay. A laboratory stock of rgRSV244 (18) was propagated in HEp-2 cells, and RSV infectivity was determined by plaque assay. hAEC cultures were exposed to 2×10^5 PFU influenza virus Udorn (multiplicity of infection [MOI] of apical cells = 1) or 1×10^6 PFU rgRSV244 (MOI of apical cells = 5) or mock treated for 2 h and harvested after 24 and 48 h of incubation, respectively. The hAEC cultures originated from two different donors (D1 and D2). For the infected cultures, we used two from each donor (i.e., a total of four cultures for each virus, two from D1 and two from D2). All the control samples were of D1 origin. The unsupervised hierarchical clustering analysis (Fig. 1A) clustered all the control samples together regardless of time of analysis (24 h or 48 h after infection). The unsupervised analysis clustered RSV and influenza virus in separate groups regardless of donor origin. mAEC cultures derived from BALB/c WT, IFNAR$^{-/-}$, and STAT1$^{-/-}$ mice were exposed to 2×10^5 PFU influenza virus WSN for 2 h or mock inoculated and harvested 24 h postinfection. Controls were run using human bronchial epithelial cells and murine AECs stimulated with UV-inactivated RSV and UV-inactivated influenza virus, and these samples were not significantly different from mock-infected samples, as determined by tumor necrosis factor alpha enzyme-linked immunosorbent assay (TNF-α ELISA), interleukin 8 (IL-8) ELISA, and interferon bioassay.

AEC histology. Influenza virus- and RSV-infected cultures were fixed in 10% paraformaldehyde. Influenza virus was visualized using goat anti-H3N2 (Meridian) and fluorescein isothiocyanate (FITC)-conjugated donkey anti-goat (Santa Cruz Biotechnology). RSV was visualized using FITC-conjugated goat anti-RSV (Virostat). For transmission electron microscopy analysis, cultures were fixed for 1 h at room temperature with 2% paraformaldehyde-2.5% glutaraldehyde in 100 mM phosphate buffer, pH 7.2. After washing in phosphate buffer, the cells were postfixed for 1 h at room temperature in 1% osmium tetroxide. After embedding in Embed 812 resin, sections were cut, stained with 2.5% uranyl acetate and 0.66% lead citrate, and viewed on a Hitachi H7650 transmission electron microscope.

RNA extraction and real-time PCR. RNA was isolated from the AEC cultures after direct lysis of cells with TRIzol (Invitrogen) and application of the resulting aqueous phase to Qiagen RNeasy Mini Columns. Two

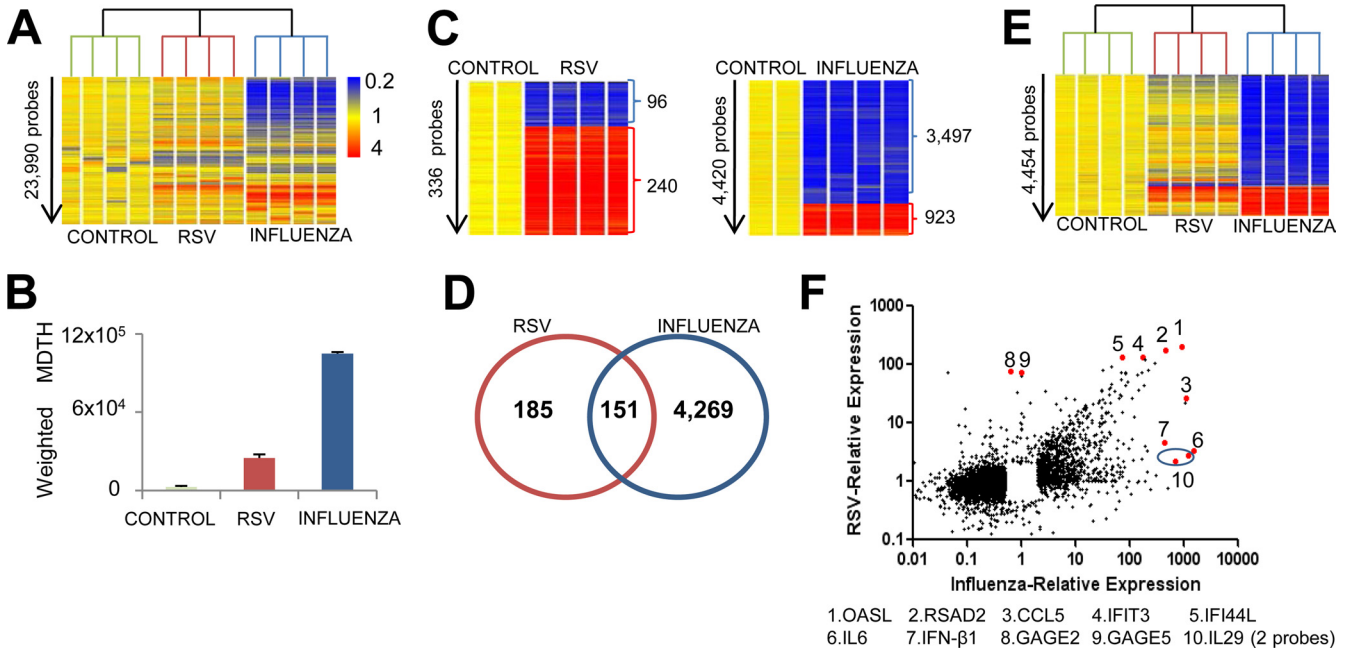

FIG 1 Primary hAECs have a distinct transcriptional signature during RSV and influenza virus infection. Primary well-differentiated, polarized, ciliated hAEC cultures were infected with influenza A virus or RSV or mock treated. The cultures originated from two different donors. Total RNA was analyzed using Illumina-HTv12 v3.0 microarrays. (A) Unsupervised hierarchical clustering of transcripts and samples segregated hAECs into three distinct groups: controls, RSV infected, and influenza virus infected. (B) The MDTH was compared between experimental groups. The error bars indicate SD. (C) Heat maps of DEGs during RSV and influenza virus infection. Supervised analysis was performed using statistical filtering ($P < 0.05$; Benjamini statistical correction; 2-fold change). The numbers of upregulated and downregulated transcripts are indicated. (D) Venn diagram showing the common and virus-specific transcripts for each infection compared to noninfected controls. (E) Gene tree comparing the expression levels of the 4,454 virus-specific DEGs after normalization to their own controls. (F) Scatter plot of the relative expression of DEGs in influenza virus- and RSV-infected hAECs. The identities of representative upregulated DEGs are indicated.

micrograms of total RNA was reverse transcribed in a 20-μl volume using an Applied Biosystems high-capacity reverse transcription kit. mRNA expression was determined for 1 μl of cDNA with the Prism 7500 sequence detection system (Applied Biosystems) using SYBR green dye and gene-specific primers designed using Primer Express software. Primer sets for the P protein of RSV were 5′ AGTGCAGGACCTACATCTGCTC (F) and 5′ AGCTGTTGGCTATGTCCTTGG (R), while for the NP protein of influenza virus they were 5′ CCAGGAAATGCTGAGATCGAAG (F) and 5′ TACACACAGGCAGGCAGACAAG 3′ (R). Data were normalized to glyceraldehyde-3-phosphate dehydrogenase (GAPDH), for which the set of primers we used was 5′ GCAAATTCCATGGCACCGT (F) and 5′ TC GCCCCACTTGATTTTGG (R). The fold increase in mRNA expression was determined using the $\Delta\Delta C_T$ method with mock-treated cultures as calibrators.

Microarray data analysis. Total RNA harvested from quadruplicate hAEC cultures was hybridized using both Illumina HT12 v3.0 expression bead chip and Agilent 014850 Whole Human Genome Microarray 4×44k G4112F(1 color). Total RNA from triplicate mAEC cultures was hybridized using an Agilent 014868 Whole Mouse Genome Microarray 4×44k G4122F (1 color). Total RNA from PBMCs was hybridized using Affymetrix HG-U133 plus 2.0 arrays. The Agilent human and mouse arrays were done at the Biomedical Genomics Core at Nationwide Children's Hospital, while the Illumina HT12 v3.0 and the Affymetrix HG-U133 plus 2.0 arrays were performed at Baylor Institute for Immunology and Research. GeneSpring GX version 7.3.1 (Agilent Technologies) was used for data visualization and analysis. For the Illumina arrays, all signal intensity values less than 10 were set to equal 10. Next, per-gene normalization was applied by dividing the signal intensity of each probe in each sample by the median intensity for that probe across the median of the control group. These normalized data were used for all downstream analyses except the assessment of molecular distance to health (MDTH), for which we used raw expression values (detailed below). Using GeneSpring, all transcripts were filtered first to select detected transcripts, i.e., those called "present" in greater than 1% of all samples (present in at least one sample; PALO). Present calls were selected if the signal precision was less than 0.01.The remaining transcripts were filtered to select the most variable probes, i.e., those that had a minimum of 2-fold expression change compared with the median intensity across all samples in greater than 1% of all samples (quality control [QC] gene list) (3). We next performed unsupervised analysis with GeneSpring using hierarchical clustering. Individual samples were grouped into horizontally presented clusters on the basis of the similarity of their expression profiles. For this stage, we based the clustering algorithm on rank correlation to distance. By examining the cluster membership, we assessed whether the samples grouped according to known factors (infection with influenza virus, RSV, or control). For the Agilent and Affymetrix arrays, we filtered transcripts that were present in at least 75% of each cohort (controls or virus-treated samples), and from these we used the transcripts that were present in either gene list (the QC gene list) as described previously (41). Supervised statistical analysis was performed starting from the QC list using a false-discovery rate with a P value of <0.05 with Benjamini multiple statistical corrections and 2-fold change. Only for the WT, IFNAR$^{-/-}$, and STAT1$^{-/-}$ comparison were the parameters loosened ($P < 0.05$, no Benjamini multiple correction, and 2-fold change).

The MDTH was calculated as previously described (35) to convert transcript abundance values into a representative score indicating the degree of transcriptional perturbation of a given sample compared with a healthy control. This approach essentially consists of carrying out outlier analyses on a gene-by-gene basis, where the dispersion of the expression values found in the baseline samples (controls) are used to determine

whether the expression value of a single case sample lies inside or outside 2 standard deviations of the controls' mean. This analysis was performed by merging the transcripts from the QC list (see above), which accounted for 23,990 probes. The distance of each sample from the uninfected control baseline was calculated as follows. In step 1, the baseline was established; for each gene, the average expression level and standard deviation of the uninfected control group were calculated. In step 2, the "distance" of an individual gene from the baseline was calculated; the difference in raw expression level from the baseline average of a gene was determined for a given sample, and then the number of standard deviations from baseline levels that the difference in expression represented was calculated. In step 3, filters were applied; qualifying genes must differ from the average baseline expression by at least 200 and 2 standard deviations. In step 4, a global distance from baseline was calculated; the number of standard deviations for all qualifying genes was added to yield a single value, the global distance of the sample from the baseline.

Supervised analysis was performed using statistical filtering in GeneSpring. The filtered list of transcripts generated for unsupervised analysis was used as the starting point for the supervised analysis, that is, those transcripts that were both detected and had at least a 2-fold change in expression compared with the median in greater than 1% of all samples. These transcripts were then tested using the Welch *t* test for comparisons across all study groups, with a false-discovery rate of 5% ($P < 0.05$). Adjustment for multiple testing was applied using the Benjamini-Hochberg multiple statistical correction.

Signaling pathway analysis was performed with Ingenuity pathway analysis (Ingenuity Systems). Canonical pathway analysis identified the pathways that were most significantly represented in the data set. The significance of the association between the data set and the canonical pathway was measured using Fisher's exact test to calculate a *P* value representing the probability that the association between the transcripts in the data set and the canonical pathway was explained by chance alone, with a Benjamini-Hochberg correction for multiple testing applied.

Transcriptional modular analysis was performed as described previously (6). Transcriptional data were obtained for eight experimental groups, including systemic onset juvenile idiopathic arthritis, systematic lupus erythematosus, liver transplant recipients, melanoma patients, and patients with acute infections (*Escherichia coli*, *Staphylococcus aureus*, and influenza A virus). For each group, transcripts with an absent flag call across all conditions were filtered out. The remaining genes were distributed among 30 sets by hierarchical clustering (*k*-means algorithm; clusters C1 through C30). The cluster assignment for each gene was recorded in a table, and distribution patterns across the eight diseases were compared among all the genes. Modules were selected using an iterative process starting with the largest set of genes that belonged to the same cluster in all study groups (that is, genes that were found in the same cluster in eight of the eight groups). The selection was then expanded to include genes with 7 of 8, 6 of 8, and 5 of 8 matches to the core reference pattern. The resulting set of genes from each core reference pattern formed a transcriptional module and was withdrawn from the selection pool. The process was repeated starting with the second-largest group of genes, then the third, and so on. This analysis led to the identification of 5,348 transcripts that were distributed among 28 modules. Each module was assigned a unique identifier indicating the round and order of selection (for example, M3.1 was the first module identified in the third round of selection). To present the global transcriptional changes graphically, spots were aligned on a grid with each position corresponding to a different module based on the original definition. The spot intensity indicates the percentage of differentially expressed transcripts from the total number of transcripts detected for that module, whereas the spot color indicates the polarity of the change.

Protein analysis. Cell culture supernatants were harvested from the apical and basolateral compartments of RSV- or influenza virus-infected or control AEC cultures. Multiplex analysis was performed using the Procarta Cytokine kit on a Luminex platform (Affymetrix Inc.). Protein concentrations were normalized to adjust for the large difference in volume between the apical (200 μl for hAECs and mAECs) and the basal (1,500 μl for hAECs and 2,000 μl for mAECs) chambers.

Microarray data accession numbers. Gene expression data from these studies can be accessed at GEO (http://www.ncbi.nlm.nih.gov/geo/query/acc.cgi?acc=GSE32140) under accession number GSE32140 for the superseries, which is composed of subset series with accession numbers GSE32137 to GSE32139 and GSE34205.

RESULTS

AECs exhibit a virus-specific transcriptional signature during infection. Primary airway cell cultures provide a system that is a good representation of the *in vivo* airway epithelial microenvironment (9, 12, 43). Primary hAEC and mAEC cultures were grown to form a well-differentiated, polarized, ciliated, pseudostratified epithelium (see Fig. S1A in the supplemental material). Primary hAEC cultures were inoculated with influenza A virus (2×10^5 PFU) or with RSV (1×10^6 PFU). Total RNA was isolated 24 h postinfection (influenza virus-infected cultures and mock-infected controls) or 48 h postinfection (RSV-infected cultures and mock-infected controls) and analyzed using microarrays. A larger viral inoculum and later collection time were used for RSV because in similar experiments in which we collected RNA at 24 h, the RSV-infected samples did not cluster separately from the mock-infected control hAEC samples (data not shown). Detection of viral antigens by immunohistochemistry showed that approximately 50% of hAECs were infected with influenza virus or RSV at 24 and 48 h, respectively (see Fig. S1B in the supplemental material). Desquamated epithelial cells were present in the influenza virus-infected samples but not in the RSV-infected samples. Quantitative PCR (qPCR) analysis corroborated that RSV- and influenza virus-infected AEC cultures had similar amounts of viral RNAs under our experimental conditions (see Fig. S1C in the supplemental material).

To validate the microarray data and to minimize false readings, RNA was analyzed in duplicate using two different platforms, Illumina HT-12 v3.0 expression bead chip and Agilent 014850 Whole Human Genome Microarray 4×44k G4112F (1 color) (see Fig. S1D in the supplemental material). The hAEC data presented below are derived from Illumina expression arrays unless otherwise indicated. To determine the transcriptional response of hAECs to RSV and influenza virus infection, we started by comparing genome-wide gene expression in infected cells and mock-infected controls. By using unsupervised hierarchical clustering of transcripts and samples based on the quality control gene list (23,990 genes), the individual samples segregated into three distinct groups that corresponded with the three experimental conditions: control, RSV, and influenza virus (Fig. 1A). The greater distance of influenza virus samples from mock samples in the condition tree compared to RSV samples suggested that the transcriptional changes on hAECs were more prominent during influenza virus infection than during RSV infection. To measure the magnitude of the gene expression changes induced by each viral infection, we converted transcript abundance into MDTH, a representative score indicating the degree of transcriptional perturbation for a given sample compared to its control (35). MDTH values were higher in influenza virus-infected hAECs than in those infected with RSV (Fig. 1B), consistent with the transcriptional perturbation of hAECs being more pronounced for infection with influenza virus than for infection with RSV.

To identify the most significant transcripts that were differen-

tially expressed between infected and control hAECs, we performed a supervised analysis under stringent conditions (pairwise comparisons with the Welch *t* test with a *P* value of <0.05, Benjamini-Hochberg multiple statistical correction, and $\geq$2-fold change). The statistical group comparisons of samples with influenza virus and controls yielded 4,420 DEGs, 923 (21%) of which were relatively overexpressed and 3,497 (79%) or which were underexpressed during influenza virus infection (Fig. 1C; see Table S1A in the supplemental material). Among the induced DEGs were those encoding interferons, i.e., IFN-A7, IFN-A14, IFN-A16, IFN-B1, IL-28B, and IL-29, with changes up to ~1,500-fold; interleukins, such as IL-1A, IL-1B, IL-23A, IL-17C, and IL-32, with changes up to ~600-fold; interferon-induced genes, such as those encoding TC-PTP, STAT1, IFI6, IFIT1, IFIT3, IFI44L, OAS1, MX1, PSMB8, TAP1, JAK2, and SOCS1, with changes up to ~130-fold; chemokines, such as CCL2, CCL3, CCL5, CCL8, CCL22, CXCL9, CXCL10, CXCL11, CXCL16, and CX3CL1, with changes up to ~80-fold; cytokines, such as TNF, CSF2, and CSF3; innate sensors and adaptor molecules, like TLR2, TLR3, NOD1, and MYD88; and apoptosis-related genes, like CASP1, CASP8, and CHEK2. Overall, hAEC samples infected with influenza virus displayed a prominent type I and type III interferon signature. The downregulated DEGs included mostly genes associated with basic metabolic pathways, such as fatty acid metabolism (ADH1C, ADH1A, ACAD10, ACADM, ALDH3A2, and CYP2A6), amino acid metabolism (AUH, BCAT2, BCKDHA, DBT, ECH, and MUT), carbohydrate metabolism (ALDH1A3, ALD3A2, ALDH4A1, ALDH5A1, ALDH6A1, and BCAT2), pyruvate metabolism (ACACA, ACACB, PCK2, and ME1), and glutathione metabolism (GCLC, GSTA2, GSTA4, and GSTA5).

When we compared RSV samples to their controls using the statistical parameters described above, we identified a total of 336 DEGs, of which 240 (71%) were upregulated and 96 (29%) were downregulated (Fig. 1C). The upregulated DEGs included type I interferon-inducible genes, such as those encoding IFI44L, IFIT2, OAS3, MX2, IFI27, OAS1, IRF7, STAT1, IFI35, and ISG20; chemokines, like CXCL10 and CCL5; cytokines, such as TNFSF13B; cell cycle-related genes (XAF1); and members of the GAGE family (see Table S1B in the supplemental material). Only two transcripts were induced more than 100-fold: CXCL10 and OASL. The number of upregulated genes in hAEC cultures exposed to RSV was 75% less than in influenza virus-infected cultures, and the number of downregulated transcripts was 96% less.

In order to dissect common and unique signatures of infection in hAECs, we compared the transcripts differentially expressed between the two viral infections and their respective controls (Fig. 1D). The majority of the DEGs were unique to each infection (4,269 transcripts were unique for influenza virus and 185 were unique for RSV), and the majority of the transcripts modulated during influenza virus infection were not altered in the RSV samples. We used these virus-specific DEGs to generate a gene tree signature that underscores differences in the responses of hAECs to each infection (Fig. 1E). A scatter plot of all the upregulated and downregulated transcripts for both infections is presented in Fig. 1F. Most of the transcripts in the influenza virus samples were downregulated, suggesting a global host cell transcriptional shutoff due to influenza virus replication. Interestingly, overexpression of type III interferons (IL-28A, IL-28B, and IL-29) was exclusive to influenza virus-infected hAECs (see Table S1C in the supplemental material). Other DEGs that were specifically induced by influenza virus and not by RSV were those encoding interleukins, such as IL-6, IL-1A, IL-1B, IL-23A, IL-17C, and IL-32; interferons and interferon-induced genes, such as IFN-B1, RSAD2, IFIT1, and IFIT3; chemokines, such as CCL2, CCL8, and CXCL5; and other cytokines, such as TNF, TNFAIP3, and TBFAIP6. The hAEC response to RSV was subtler but contained unique DEGs, such as members of the GAGE family (GAGE1, GAGE4, and GAGE5) (see Table S1D in the supplemental material). Altogether, these observations indicate that the response of hAECs during RSV and influenza virus infection was largely virus specific and that the response to influenza virus was more robust and diverse than that to RSV infection.

A common type I interferon signature. First, the supervised statistical analysis of the hAEC response to RSV and influenza virus showed a gene signature with 151 common genes (Fig. 1D), and these common DEGs followed similar patterns of expression (Fig. 2A). The majority of overexpressed DEGs were type I interferon associated, such as the interferon-inducible IFI27, IFI44L, OAS21, OAS2, OAS3, STAT1, MX2, IFIH1, IFITM2, IFITM3, ISG20, IRF7 and IRF1 genes and genes for interferon-induced chemokines CXCL10, CCL5, CXCL11, CXCL9, CCL20, and IL-8 (CXCL8); members of the HLA complex (HLA-E, HLA-A, and HLA-F); proapoptotic molecules (CASP1 and CASP8); immune-inhibitory genes (SOCS2); and extracellular matrix metallopeptidases (MMP13 and ADAM8) (see Table S2A to E in the supplemental material). These findings suggested that the core of the hAEC response during influenza virus and RSV infection was type I interferon dependent. The majority of the common DEGs followed similar patterns of expression, but the changes were larger in response to influenza virus than in response to RSV. Second, Ingenuity pathway analysis confirmed interferon signaling and activation of interferon-regulated factors by cytosolic pattern recognition receptors as two significantly overrepresented pathways in both RSV- and influenza virus-infected samples (see Fig. S2 in the supplemental material). Genes downstream of type I IFN-α/β receptor signaling were significantly overrepresented in hAECs infected with both viruses (Fig. 2B), and IRF7 was at the center of the hAEC response to RSV and influenza virus (see Fig. S2B and D in the supplemental material). These analyses also uncovered differences in the numbers and the changes of the genes involved in the type I interferon response to both infections, with more transcripts participating and presenting greater changes in the influenza virus samples than in those from RSV. Third, we used a transcriptional modular framework analysis (6) to obtain a virus-specific signature of the hAEC response (Fig. 2C). The interferon module (M3.1) was the only common module with upregulated transcripts for both viruses, albeit with greater intensity in the influenza virus samples than in the RSV samples. More modules were altered for influenza virus than for RSV, confirming again that more pathways were altered by influenza virus than by RSV. Most of the modules in the hAEC samples infected with influenza virus were downregulated, which correlated with the large number of downregulated DEGs (Fig. 1C). Altogether, these three independent strategies for the analysis of signaling pathways revealed that hAECs reacted to viral infection through a central type I interferon-mediated response, which was more robust in the case of influenza virus than in the case of RSV.

Protein validation of microarray results and polarized cytokine secretion by hAECs. To validate the microarray data, we measured protein contents in the apical and basal supernatants of

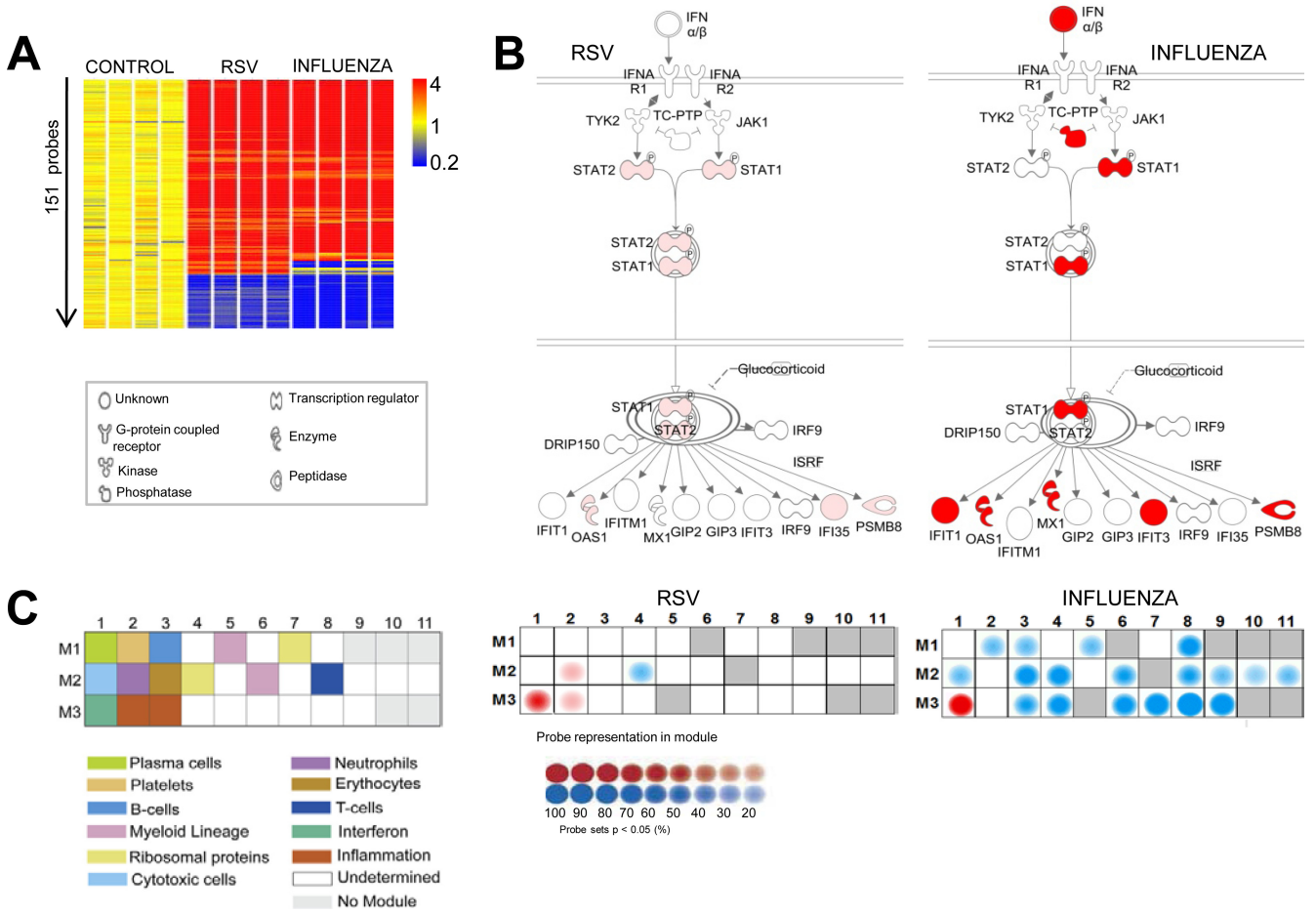

FIG 2 A common type I interferon-inducible signature in primary hAECs infected with RSV or influenza virus. (A) Comparison of the signature with 151 common genes among control and influenza virus- and RSV-infected hAECs. (B) Ingenuity pathway analysis (Fisher test, $P < 0.05$) revealed an interferon signaling canonical pathway in both infections. Different color intensities of ingenuity symbols indicate different levels of gene expression. Darker red indicates increased expression. (C) Transcriptional modular framework analyses of hAECs infected with RSV and influenza virus. To present the transcriptional changes graphically, the spots are aligned on a grid, with each position corresponding to a different functional module based on the original definitions (6). The spot intensity indicates the percentage of differentially expressed transcripts among the total number of transcripts detected for that module, whereas the spot color indicates the polarity of the change (red is upregulated, and blue is downregulated).

hAEC cultures and compared it to the relative changes in gene transcription. Of the cytokines that were highly expressed in influenza virus by microarray, IL-1α, IFN-β1, IL-6, and IL-8 (CXCL8) were also present in culture supernatants (Fig. 3A; see Fig. S3A and B in the supplemental material). IL-6 and IL-8 were also detected in the supernatants from RSV-infected hAECs, although in smaller concentrations than in the influenza virus samples. Granulocyte colony-stimulating factor (G-CSF) and macrophage colony-stimulating factor (M-CSF) were produced in significant amounts by influenza virus- and RSV-infected hAECs. The analysis of chemokine expression revealed the breadth of the response to influenza virus compared to RSV infection (Fig. 3B; see Fig. S3C and D in the supplemental material). Of the CCL chemokines, influenza virus infection induced the expression of CCL2 to -5, CCL7 to -8, and CCL22 from 10- to 1,000-fold (100 to 20,000 pg). RSV infection exclusively induced the production of CCL5, and to a lesser extent than in the influenza virus-infected hAEC cultures. Of the CXCL chemokines, both viruses induced CXCL9, CXCL10, and CXCL11, while CXCL2, CXCL5, and CXCL13 were more prominent in the influenza virus samples. Importantly, the majority of cytokines and chemokines produced by hAECs were detected in larger quantities in the basal than in the apical supernatants. This observation indicates a strong basolateral polarization of the cytokine and chemokine secretion by primary differentiated hAECs in response to respiratory virus infection. Altogether, these data indicated that the production of immune mediators was more robust and diverse in the hAEC cultures infected with influenza virus than in those infected with RSV.

Critical role of the IFNAR/STAT1 axis in the response of AECs to viral infection. To determine the impact of interferons on the response of AECs to respiratory virus infection, we analyzed the response to influenza virus infection using mAECs deficient in IFNAR signaling (which lack type I interferon signaling) or in STAT1 signaling (which lack signaling by most interferons). We used influenza virus for these experiments, but not RSV, because RSV fails to efficiently infect the murine bronchiolar epithelium (37). First, we validated the mAEC model of influenza virus

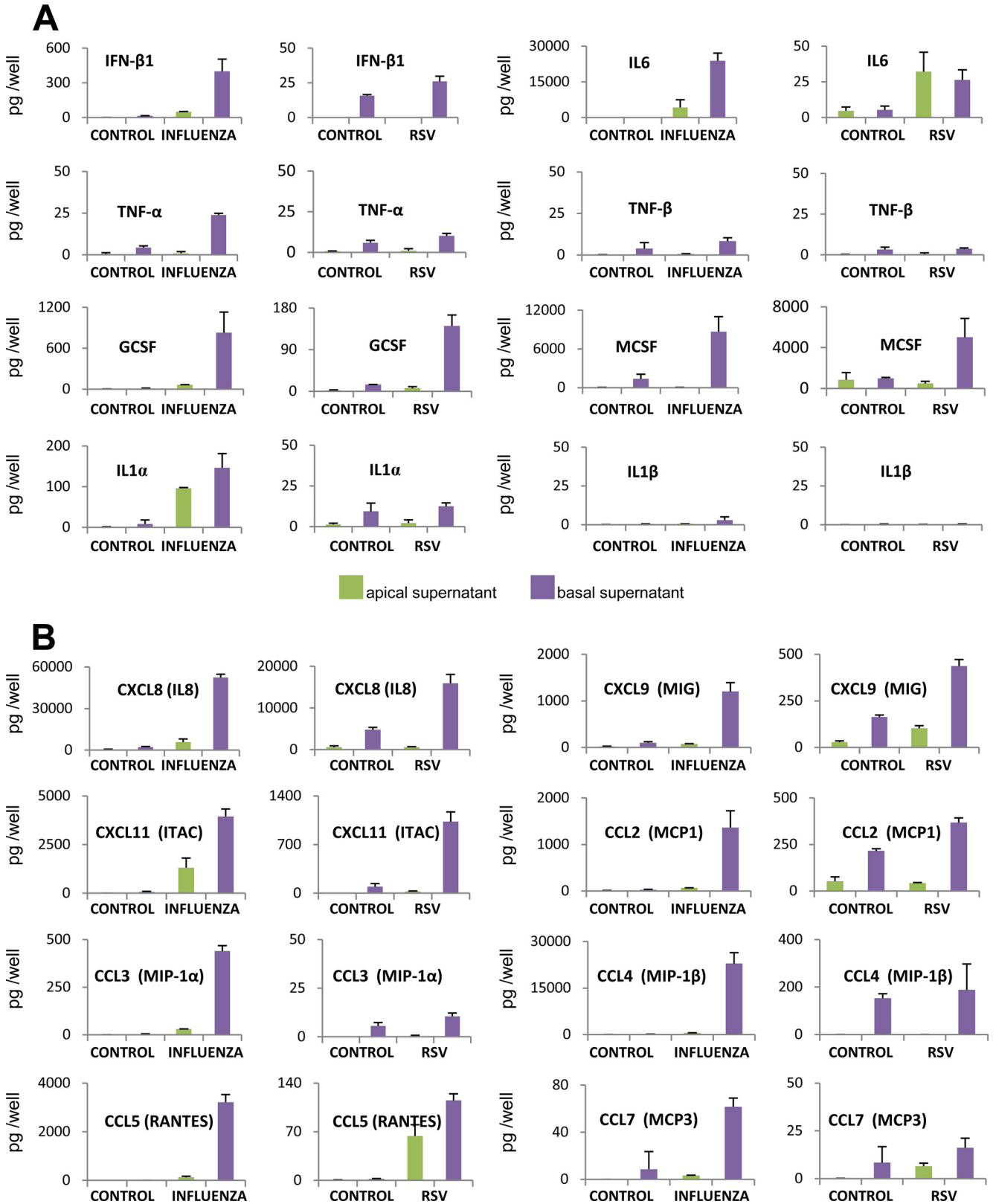

FIG 3 Basolateral polarization of cytokine and chemokine secretion in primary hAECs infected with RSV or influenza virus. Cell culture supernatants were harvested from the apical and basolateral compartments of RSV- or influenza virus-infected or control AEC cultures. Multiplex analysis was performed on a Luminex platform. Protein concentrations were normalized to the volume of the apical (200-μl) and the basal (1,500-μl) chambers. (A) Cytokines in the apical and basolateral supernatants of hAEC cultures. The error bars indicate SD. (B) Chemokines in the apical and basolateral supernatants of hAEC cultures. The error bars indicate SD.

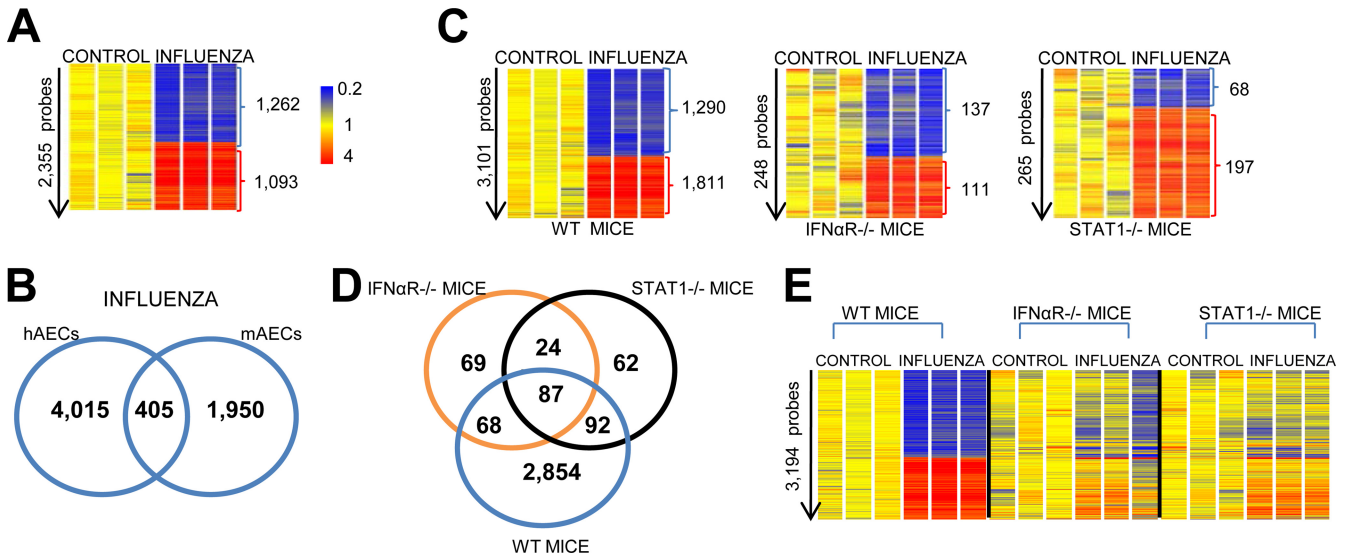

FIG 4 Transcriptional signature of influenza virus infection in primary mAECs derived from wild-type, IFNAR$^{-/-}$, or STAT1$^{-/-}$ mice. Primary well-differentiated, polarized, ciliated mAEC cultures were infected with influenza A virus or mock treated. Total RNA was analyzed using Agilent 014868 Whole Mouse Genome Microarray 4×44k G4122F (1 color). (A) Heat map of DEGs during influenza virus infection of mAECs. Supervised analysis was performed using statistical filtering ($P < 0.05$; Benjamini statistical correction; 2-fold change). The numbers of upregulated and downregulated transcripts are indicated. (B) Venn diagram showing the common and species-specific transcripts for human and murine AECs during influenza virus infection. A human strain of influenza A virus (Udorn) was used to infect human AECs, and a mouse-adapted influenza virus strain (WSN) was used to infect mouse AECs. (C) Comparison of the heat maps of DEGs during influenza virus infection of wild-type, IFNAR$^{-/-}$, and STAT1$^{-/-}$ mAECs. Supervised analysis was performed using less stringent statistical filtering ($P < 0.05$; 2-fold change) than for panel A. The numbers of upregulated and downregulated transcripts are indicated. (D) Venn diagram showing the common and strain-specific transcripts for mAECs of wild-type, IFANR$^{-/-}$, or STAT1$^{-/-}$ origin during influenza virus infection. (E) Gene tree comparing the expression levels of the 3,194 influenza virus-specific DEGs in mAECs of wild-type, IFANR$^{-/-}$, or STAT1$^{-/-}$ origin after normalization to their own noninfected controls.

infection. Triplicate primary mAEC cultures were mock infected or infected with influenza virus for 24 h. Pairwise comparison between the two conditions using the statistical parameters described previously for hAECs yielded 2,355 DEGs, of which 1,093 were upregulated and 1,262 were downregulated (Fig. 4A). Interferons (IFN-B1, IFN-A1, IFN-A16, and IL-28B) and interferon-inducible genes (RSAD2, IFIT2, IFI44L, IFIT3, OAS3, IlGP1, GIVIN1, CXCL11, CXCL10, CCL10, and CXCL9) represented the largest category of overexpressed DEGs (see Table S3A in the supplemental material). Next, we compared the responses of hAECs and mAECs during influenza virus infection. This analysis revealed that 405 DEGs were common to hAECs and mAECs (Fig. 4B). This common AEC signature to influenza virus infection included interferons (IFN-B1, IFN-A16, and IL-28B), interferon-inducible genes (IFI44L, IFIT3, IFIT1, OAS1, OAS2, OAS3, MX1, MX2, IRF7, IFI44, STAT1, and RSAD2), interferon-induced chemokines (CXCL11, CCL5, CXCL10, CXCL9, and CCL20), interleukins (IL17C and IL1A), pathogen recognition receptors (TLR2, TLR3, and NOD2), and immunoregulatory factors (IDO1 and SOCS1) (see Table S3A and B in the supplemental material). Altogether, these results reveal the similarities between the responses of human and murine primary AECs to different strains of influenza virus and highlight the fact that even though the overall response was less robust in mAECs than in hAECs, both species of AECs displayed a prominent type I and type III interferon signature. To determine whether interferons were essential for the epithelial cell response to influenza virus infection, we performed a supervised analysis using pairwise comparisons to identify the most significant transcripts that were differentially expressed in the presence or absence of IFNAR or STAT1 signaling. When we applied the same statistical parameters previously used with hAECs and mAECs (pairwise comparisons with the Welch *t* test with a *P* value of <0.05, Benjamini-Hochberg multiple statistical correction, and ≥2-fold change), the number of DEGs after influenza virus infection in IFNAR$^{-/-}$ and STAT1$^{-/-}$ mAECs was zero. This finding highlighted the essential role of the IFN-α/β–STAT1 axis in the transcriptional response of AECs to influenza virus.

To dissect which transcripts could potentially play a role in the anti-influenza virus response of mAECs in the absence of IFNAR and STAT1 signaling, we loosened the statistical parameters (pairwise comparisons by the Welch *t* test with a *P* value of <0.05 and ≥2-fold change). This analysis resulted in 3,101 DEGs in WT mAECs, of which 1,811 were upregulated and 1,290 were downregulated between control and influenza virus-infected mAECs (Fig. 4C). IFNAR$^{-/-}$ mAECs had 248 DEGs (111 upregulated and 137 downregulated). STAT1$^{-/-}$ mAECs showed 265 DEGs (197 upregulated and 68 downregulated). Lack of IFNAR or STAT1 signaling resulted in an ~10-fold reduction in the magnitude of the mAEC response to influenza virus. A combined list of the 50 most highly up- and downregulated DEGs in IFNAR$^{-/-}$ and STAT1$^{-/-}$ mAECs is shown in see Table S4A and B in the supplemental material. In the absence of IFNAR signaling, an interferon-inducible signature was still apparent (IFN-B1, IL-28B, IFI203, IFIT3, OASL, CXCL11, CXCL3, CCL5, CXCL1, and CXCL2), although of reduced magnitude (maximum change, 38-fold). STAT1-deficient mAECs also displayed an interferon-inducible signature (IFN-B1, IFI203, IFIT3, RSAD2, CXCL10, CXCL3,

CXCL2, CCL5, and CCL20) of lower intensity (maximum change, 58-fold) in response to influenza virus infection. In order to elucidate which transcripts were implicated in the mAEC response to influenza virus in the absence of IFNAR or STAT1 signaling, we performed a comparison of the common DEGs in WT, IFNAR$^{-/-}$, and STAT1$^{-/-}$ mAECs. The common signature of influenza virus infection contained 87 transcripts (Fig. 4D), including type III interferon (IL-28); interferon-inducible genes, such as OASL1, OASL, RSAD2, and IFIT3; chemokines (CXCL10, CXCL2, CCL5, and CCL20); and interleukins and interleukin-inducible genes (IL17C, IL4L1, and IL1RL1) (see Table S4C in the supplemental material). A gene tree combining all the common and unique DEGs for each type of mAEC shows the reduction of the transcriptional response to influenza virus infection when there is no signaling through IFNAR or STAT1 (Fig. 4E). Although the common transcripts among WT, IFNAR$^{-/-}$, and STAT1$^{-/-}$ mAECs followed identical patterns of expression, the fold changes were more robust in WT mAECs (e.g., CXCL10 was ~138-fold upregulated in WT, ~16-fold in IFNAR$^{-/-}$, and ~20-fold in STAT1$^{-/-}$ mAECs). Our analysis identified genes encoding molecules closely associated with the interferon signaling pathways in all mAECs, although NF-κB appeared at the center of the molecular signature in IFNAR$^{-/-}$ and STAT1$^{-/-}$ mAECs (see Fig. S4 in the supplemental material). A comparison of the relative changes in gene transcription with the protein analysis of immune mediators in culture supernatants corroborated the finding that the immune response of mAECs to influenza virus was significantly reduced in the absence of IFNAR and STAT1 signaling, although it was not completely abrogated in all instances (KC, LIX, MIP-2, and TNF-α) (Fig. 5; see Fig. S5 in the supplemental material). This analysis with mAECs also corroborated the strong basolateral polarization of the cytokine and chemokine secretion by the airway epithelium.

Correlation of molecular signatures between the airway epithelium and peripheral blood. To understand whether respiratory viruses elicit common or unique transcriptional signatures across different cell populations and to determine to what extent the systemic response in peripheral blood correlates with the initial response at the mucosal site of infection, we performed genome-wide transcriptional-profile analyses in PBMCs isolated from patients with acute RSV bronchiolitis or acute influenza virus infection and from healthy controls. The demographics of the patient population are shown in Table S5 in the supplemental material. A distinct transcriptional signature was defined in patients with acute influenza or acute RSV infection by using a combination of probe expression level, statistical filters, and hierarchical clustering (Fig. 6A). The statistical group comparisons of patients with influenza virus infection and healthy controls yielded 142 DEGs, of which 91 were overexpressed and 51 were downregulated during acute influenza virus infection (see Table S6A in the supplemental material). Among the induced DEGs, there were many interferon-inducible transcripts, such as IFI27, IFI44L, IFI44, IFIT3, OAS1, OAS2, OAS3, OASL, MX1, MX2, G1P2, and DEFA1 (with changes ranging from 80- to 2-fold). Group comparisons of patients with confirmed RSV infection and healthy controls yielded 110 DEGs, of which 78 were overexpressed and 32 were downregulated during acute RSV infection (see Table S6B in the supplemental material). Among the RSV-induced DEGs were the interferon-inducible IFI27 (38-fold change) and DEFA1, DEFA3, SN, and IL-1RN (changes from 12- to 2-fold). The PBMC response during RSV and influenza virus infection had a signature with 18 common interferon-inducible genes, and these common DEGs followed similar patterns of expression (Fig. 6C to E). IFI27 was the top common upregulated DEG in both cohorts of patients. Comparison of the transcriptional profiles using modular framework analysis and Ingenuity pathway analysis revealed significant differences in the magnitude of the interferon-related response between PBMCs from patients with influenza virus or RSV infection (Fig. 6F and G). Altogether, these results indicate that although the transcriptional response of PBMCs from patients with acute RSV and influenza virus infection was predominantly virus specific, it also had a common interferon-inducible signature that was more robust in patients with influenza virus infection than in those with RSV infection.

Next, we wanted to characterize the relationship between the response observed at the molecular level and the clinical outcome of the infection by comparing the transcriptional perturbation of PBMCs with the severity of the disease. To assess disease severity, we applied a score that included clinical markers of severity, such as percutaneous O_2 saturation, respiratory rate, subcostal retractions, general appearance, and auscultation. We calculated the average perturbation of the overexpressed DEGs in PBMCs of patients with acute RSV infection or influenza and found that it correlated with the clinical score for disease severity (Fig. 6H to J). This analysis indicates that there is an association between the degree of molecular perturbation in PBMCs from patients with RSV bronchiolitis or with acute influenza virus infection and the severity of the clinical manifestations in each cohort of patients.

To identify common functional components of the transcriptional host response in the airway epithelium and in peripheral blood, we compared the DEGs that were coordinately expressed in hAECs and PBMCs during the response to RSV or influenza virus infection. The response to influenza virus in hAECs and PBMCs had a signature with 36 common genes (Fig. 7A) that included numerous interferon-inducible genes (IFI27, IFI44, IFI44L, IFIT3, ISG15, HERC5, HERC6, MX1, MX2, OAS1, OAS2, OAS3, and OASL). In addition, these influenza virus-induced common DEGs followed similar patterns of expression in hAECs and PBMCs (Fig. 7B). There was a statistically significant correlation between the expression of common DEGs induced in the airway epithelium and in PBMCs during influenza virus infection (Fig. 7C) and between the transcripts of the interferon module (Fig. 7D). When we performed a similar analysis comparing the response of hAECs infected with RSV to that of PBMCs from patients with acute RSV, we obtained 4 common DEGs (IFI27, TYMS, NDUFS1, and ZMAT3) (Fig. 7E and F). Although the majority of the transcripts induced in response to RSV infection were different in PBMCs and AECs, we investigated the possible relationship between the only four common DEGs and found a statistically significant correlation (Fig. 7G). A statistically significant correlation was also observed among the transcripts of the interferon module (Fig. 7H). Altogether, these results highlight that there is a correlation of the molecular signatures between the airway epithelium and PBMCs during the response to a respiratory virus infection. Notably, IFI27 was the only common DEG induced in response to RSV and influenza virus in both hAECs and PBMCs.

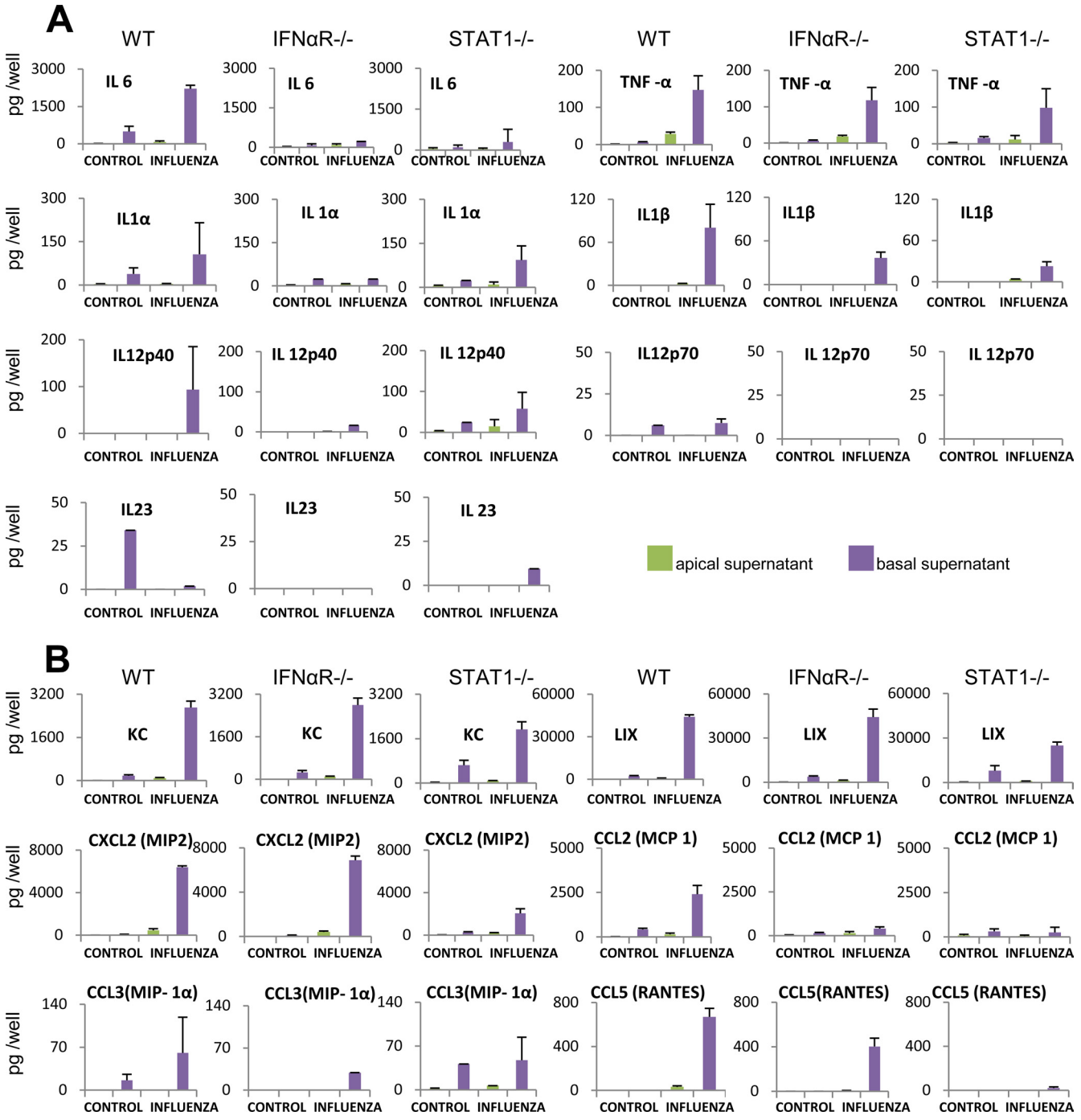

FIG 5 Reduced cytokine and chemokine secretion in primary mAECs deficient in IFNAR or STAT1 signaling during influenza virus infection. Cell culture supernatants were harvested from the apical and basolateral compartments of influenza virus-infected AEC cultures derived from wild-type, IFNAR$^{-/-}$, or STAT1$^{-/-}$ mice. Multiplex analysis was performed on a Luminex platform. Protein concentrations were normalized to the volume of the apical (200-μl) and the basal (2,000-μl) chambers. (A) Cytokines in the apical and basolateral supernatants of wild-type, IFNAR$^{-/-}$, and STAT1$^{-/-}$ mAEC cultures. The error bars indicate SD. (B) Chemokines in the apical and basolateral supernatants of wild-type, IFNAR$^{-/-}$, and STAT1$^{-/-}$ mAEC cultures. The error bars indicate SD.

DISCUSSION

How organisms respond appropriately to a wide variety of antigens and microorganisms is a central question in immunology. However, we have limited knowledge of how the epithelium of the airways responds to infection and regulates immunity at the outset of infection. We performed independent challenges of primary polarized hAECs with RSV and influenza virus and compared their antiviral responses with gene expression signatures obtained from peripheral blood of patients with RSV bronchiolitis and acute influenza virus infection. The results provide evidence that the epithelial response to RSV and influenza virus infection is quantitatively and qualitatively virus specific. Each virus induced

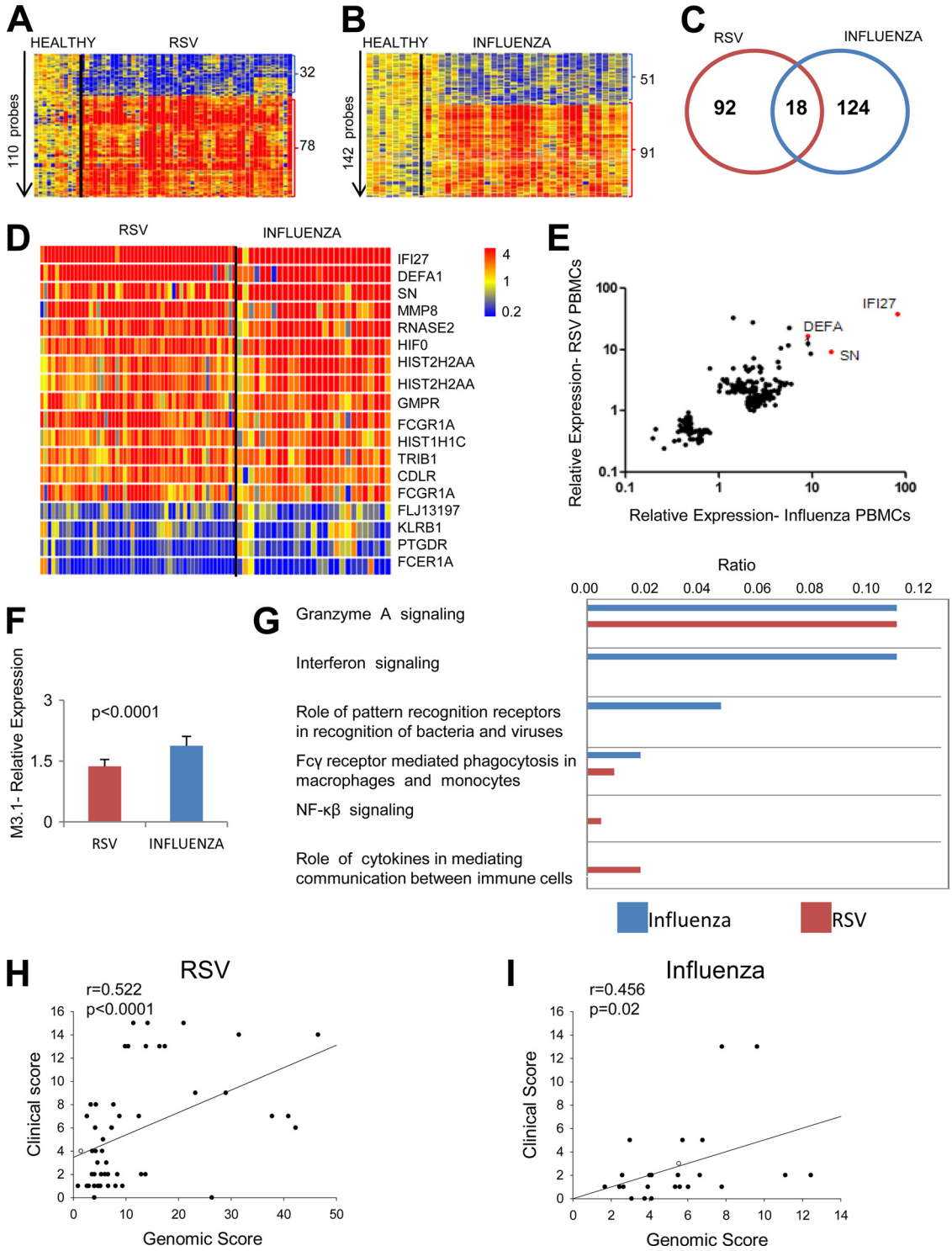

FIG 6 Molecular signatures in PBMCs from patients with acute RSV and influenza virus infection. (A) Heat map of DEGs in patients with RSV bronchiolitis compared with healthy controls. (B) Heat map of DEGs in patients with acute influenza compared with healthy controls. (C) Venn diagram showing the common and virus-specific transcripts for each infection normalized to healthy controls. (D) Comparison of the common 18-gene signature between RSV and influenza virus PBMCs. (E) Scatter plot of the relative expression of DEGs in PBMCs of influenza virus- and RSV-infected patients. The identities of representative upregulated DEGs are indicated. (F) Median expression levels of the interferon module in PBMCs from RSV- and influenza virus-infected patients. The error bars indicate SD. (G) Ingenuity pathway analysis of DEGs in PBMCs from RSV- and influenza virus-infected patients. The bars represent the frequency of transcripts from our data set that participate in the presented canonical pathway. (H) Correlation analysis of clinical score versus genomic score in PBMCs from influenza virus-infected patients. The clinical score measures disease severity in a range from 0 to 12 (see Materials and Methods). The genomic score shows the average perturbation of the upregulated DEGs. Each symbol represents a single patient. Spearman correlation, $r = 0.42$, $P \leq 0.004$. (I) Correlation analysis of clinical score versus genomic score in PBMCs from RSV-infected patients. The analysis was performed as for panel H ($r = 0.49$; $P \leq 0.018$).

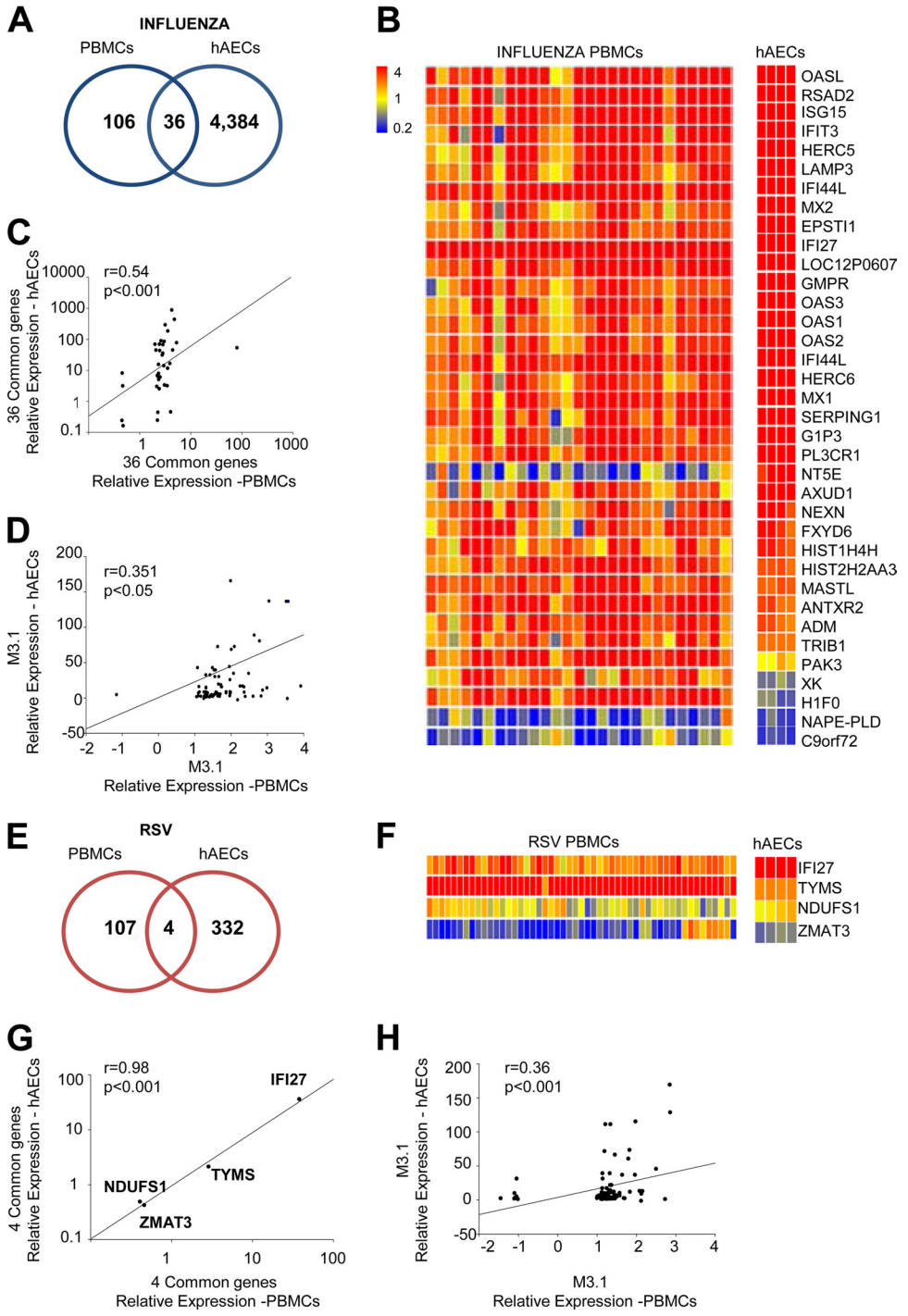

FIG 7 The transcriptional signatures induced by RSV and influenza virus correlate in hAECs and PBMCs. (A) Venn diagram showing the common and tissue-specific transcripts for influenza virus-infected samples in PBMCs and hAECs. (B) Heat map of the 36 common DEGs in PBMCs from patients with acute influenza and in influenza virus-infected hAECs. (C) Relative expression of the common DEGs in PBMCs from influenza patients and influenza virus-infected hAECs. Each symbol represents a single gene. Spearman correlation, $r = 0.54$, $P < 0.001$. (D) Relative expression of the interferon module transcripts in PBMCs from influenza patients and influenza virus-infected hAECs. Each symbol represents a single gene. $r = 0.351$, $P < 0.05$. (E) Venn diagram showing the common and tissue-specific transcripts for RSV-infected samples in PBMCs and hAECs. (F) Heat map of the 4 common DEGs in PBMCs from patients with RSV bronchiolitis and in RSV-infected hAECs. (G) Relative expression of the common DEGs in PBMCs from RSV-infected patients and RSV-infected hAECs. Each symbol represents a single gene. $r = 0.98$, $P < 0.001$. (H) Relative expression of the interferon module transcripts in PBMCs from RSV-infected patients and RSV-infected hAECs. Each symbol represents a single gene. $r = 0.36$, $P < 0.001$.

the expression of a number of common and unique DEGs, although it is formally possible that different strains of RSV and influenza virus may produce different outcomes. There was a direct and significant correlation in the common DEGs and in the interferon responses between AECs and PBMCs from patients with acute RSV or influenza virus infection. These findings provide evidence of the plasticity of the AEC response to infection and identify a correlation between the systemic immune response in peripheral blood and the immune response of the airway epithelium at the onset of infection.

The response to influenza virus displayed prominent type I and III interferon signatures, and a large variety of inflammatory cytokines and chemokines were also upregulated and secreted. This AEC response was quantitatively and qualitatively more robust and diverse than the response to RSV, which elicited a weaker response restricted to type I interferon-inducible genes and a limited production of cytokines and chemokines. It is tempting to speculate that the weak innate response of the airway epithelium to RSV may contribute to the poor systemic immunity to the virus (14, 17). Absence of epithelial proinflammatory Th1 cytokines (i.e., IL-6 and IL-1) or of type III IFNs (IL-28 and IL-29), a weak type I IFN response, and the secretion of Th1 chemokines like CCL3 and CCL5 in small amounts might restrain the activation and recruitment of immune cells to the site of infection. Thus, the inability of the epithelium to initiate a proper Th1 inflammatory response to RSV could set the background for a Th1/Th2 imbalance (39), leading to more exaggerated clinical manifestations of RSV infection, such as acute bronchiolitis or asthma in specific individuals. Although some of the observed differences in the response of AECs to RSV and influenza virus can be attributed to the cytopathic effect of influenza virus, to differences in the activity of the nonstructural (NS) proteins, or to differences in temporal kinetics and virus inoculum, the findings are noteworthy, given that both groups of hAEC cultures had similar amounts of viral RNAs and of infected cells at the time of analysis.

Transcriptional signatures of disease in peripheral blood are being used to understand pathogenesis and to improve diagnosis (3, 6, 23, 41, 58). Our analysis has identified transcriptional perturbations at the mucosal site of pathogen entry and replication that are virus specific, such as type III interferons for influenza virus-infected hAECs, which is in concordance with previous observations in mouse lungs (24). An unexpected family of tumor antigens, GAGE, was induced during RSV infection. These antiapoptotic tumor antigens are capable of interacting with IRF1 and of reducing its expression (27), which may help explain the weak interferon response observed in RSV-infected hAECs at both the transcriptional and protein levels. Our observations highlight the plasticity of the airway epithelium to elicit virus-specific immune effector responses.

We used three independent but complementary strategies (supervised, pathway, and modular framework analyses) to examine the signaling pathways involved in the response of the airway epithelium to RSV and influenza virus. These analyses revealed that hAECs respond to RSV and influenza virus infection through a predominant type I interferon-mediated response. Four pathways can mediate the AEC response to infection: (i) PKR-stress-apoptosis; (ii) NF-κB/RelA; (iii) RNA sensing, interferons, and interferon-stimulated genes; and (iv) WNT signaling (31, 32, 46). NF-κB and interferons mediate the epithelial response to RSV and influenza virus (2, 5, 29, 56). Our recent work using mouse models of infection has highlighted that interferons and epithelial cells are central players during the immune response of the airways and that different viral infections of the lung induce singular interferon responses (24, 25, 55). Evidence from the analysis of IFNAR$^{-/-}$ and STAT1$^{-/-}$ mAECs at the gene and protein levels shows a dramatic reduction of the innate effector response during influenza virus infection, corroborating that interferons and STAT1 play a central role in the initiation of immune responses by the airway epithelium. Nevertheless, the inflammatory response and the interferon signature were still present in the absence of IFNAR and STAT1 signaling. Redundant alternative pathways of either IRF3 or IRF7 induction (15, 45) and increased NF-κB activation are likely to contribute to the antiviral inflammatory response of mAECs and are revealed in the absence of normal interferon signaling.

A key finding was the strong basolateral polarization of the secretion of cytokines and chemokines by AECs during infection. This observation was reproduced in human and murine epithelial cultures and observed in response to influenza virus and RSV. The respiratory epithelium is able to induce a highly specific innate immune response to viral infection, and our findings suggest that the inflammatory mediators and chemotactic agents are mainly directed toward the lung interstitium instead of into the lumen of the airways. During the initial stages of infection, basolateral secretion of cytokines and chemokines, such as IL-8 and IL-6, by epithelial cells plays a role in attracting and activating immune cells from the lung interstitium or the circulation toward peribronchial areas, but it does not affect the cell populations located in the lumen of the airways unless the integrity of the epithelial barrier is compromised. On the other hand, apical secretion of cytokines and chemokines would lead to the recruitment of inflammatory cells into the lumen of the airways and could cause narrowing of air spaces, increased ventilation-perfusion mismatch, and deterioration of lung function (36).

AECs act as innate effectors during viral infection, and their response is largely virus specific. Because regulation of innate immunity at the point of pathogen entry may determine the subsequent host immune response and clinical outcome, we attempted to correlate the response of AECs with systemic responses. As has been shown previously in other settings (41, 58), our findings demonstrate that gene expression signatures in PBMCs discriminate between patients with acute influenza virus infection and acute RSV bronchiolitis. Although both infections cause the stimulation of interferon-inducible genes, the identity of the induced genes was largely unique for each infection, and there were also significant differences in the magnitude of the interferon-related response. IFI27 was the only transcript strongly upregulated in hAECs and PBMCs during both viral infections. IFI27 (also known as ISG12) has direct antiviral properties against many viruses (28), regulates interferon-mediated apoptosis (42), and it is the most upregulated transcript in children with RSV bronchiolitis (11). IFI27 overexpression constitutes a biomarker of viral infection in both the airway epithelium and peripheral blood.

Our results show a significant correlation in the expression of common DEGs and in the expression of interferon-related genes between hAEC and PBMC samples. The replication of RSV and influenza virus is restricted to the mucosa of the airways, but these respiratory viruses induce specific signatures of infection that are conserved across fundamentally different anatomical compartments and cell populations. Cells at the site of infection and in

peripheral blood undergo a relatively common reprogramming of their transcriptomes during infection, suggesting that pathogen-specific molecular signatures are a central component of host defense. In addition, we found that during both RSV bronchiolitis and acute influenza there was a significant correlation between the level of induction of DEGs in PBMCs and the severity of disease. Thus, the molecular signature of respiratory virus infection in peripheral blood correlated with the transcriptional signature in the airway epithelium and with the clinical severity of disease. It would be interesting for future studies to analyze the response of epithelial cells isolated from either nasal or bronchial lavage fluids of patients with viral infection and compare it with the PBMC response of the same patients. Defining biomarkers and common molecular signatures of infection in the airway mucosa and blood compartments will help to identify new correlates of protection during respiratory virus infection.

ACKNOWLEDGMENTS

We thank the Biomedical Genomics Core and the Morphology Core at Nationwide Children's Hospital and the Microarray Core at Baylor Institute for their technical help. We thank Sara Mertz for help in establishing hAEC cultures and Juanita Lozano and Evelyn Torres for their efforts with patient recruitment.

This work was supported in part by an award from Cystic Fibrosis Foundation Therapeutics, Inc. (M.E.P.), and by NIH grants AI057234 (O.R.) and AI59603 and AI082962 (E.F.), the DANA Foundation (O.R.), and The Research Institute.

REFERENCES

1. **Bals R, Hiemstra PS.** 2004. Innate immunity in the lung: how epithelial cells fight against respiratory pathogens. Eur. Respir. J. **23**:327–333.
2. **Bernasconi D, Amici C, La Frazia S, Ianaro A, Santoro MG.** 2005. The IkappaB kinase is a key factor in triggering influenza A virus-induced inflammatory cytokine production in airway epithelial cells. J. Biol. Chem. **280**:24127–24134.
3. **Berry MP, et al.** 2010. An interferon-inducible neutrophil-driven blood transcriptional signature in human tuberculosis. Nature **466**:973–977.
4. **Bertrand P, Aranibar H, Castro E, Sanchez I.** 2001. Efficacy of nebulized epinephrine versus salbutamol in hospitalized infants with bronchiolitis. Pediatr. Pulmonol. **31**:284–288.
5. **Bitko V, Barik S.** 1998. Persistent activation of RelA by respiratory syncytial virus involves protein kinase C, underphosphorylated IkappaBbeta, and sequestration of protein phosphatase 2A by the viral phosphoprotein. J. Virol. **72**:5610–5618.
6. **Chaussabel D, et al.** 2008. A modular analysis framework for blood genomics studies: application to systemic lupus erythematosus. Immunity **29**:150–164.
7. **Ciencewicki JM, Brighton LE, Jaspers I.** 2009. Localization of type I interferon receptor limits interferon-induced TLR3 in epithelial cells. J. Interferon Cytokine Res. **29**:289–297.
8. **Diamond G, Legarda D, Ryan LK.** 2000. The innate immune response of the respiratory epithelium. Immunol. Rev. **173**:27–38.
9. **Dvorak A, Tilley AE, Shaykhiev R, Wang R, Crystal RG.** 2011. Do airway epithelium air-liquid cultures represent the in vivo airway epithelium transcriptome? Am. J. Respir. Cell Mol. Biol. **44**:465–473.
10. **Fernandez-Sesma A, et al.** 2006. Influenza virus evades innate and adaptive immunity via the NS1 protein. J. Virol. **80**:6295–6304.
11. **Fjaerli HO, et al.** 2006. Whole blood gene expression in infants with respiratory syncytial virus bronchiolitis. BMC Infect. Dis. **6**:175.
12. **Fulcher ML, Gabriel S, Burns KA, Yankaskas JR, Randell SH.** 2005. Well-differentiated human airway epithelial cell cultures. Methods Mol. Med. **107**:183–206.
13. **Girard MP, Cherian T, Pervikov Y, Kieny MP.** 2005. A review of vaccine research and development: human acute respiratory infections. Vaccine **23**:5708–5724.
14. **Glezen WP, Taber LH, Frank AL, Kasel JA.** 1986. Risk of primary infection and reinfection with respiratory syncytial virus. Am. J. Dis. Child. **140**:543–546.
15. **Goodman AG, et al.** 2010. The alpha/beta interferon receptor provides protection against influenza virus replication but is dispensable for inflammatory response signaling. J. Virol. **84**:2027–2037.
16. **Hall CB, Douglas RG, Jr, Simons RL, Geiman JM.** 1978. Interferon production in children with respiratory syncytial, influenza, and parainfluenza virus infections. J. Pediatr. **93**:28–32.
17. **Hall CB, Walsh EE, Long CE, Schnabel KC.** 1991. Immunity to and frequency of reinfection with respiratory syncytial virus. J. Infect. Dis. **163**:693–698.
18. **Hallak LK, Spillmann D, Collins PL, Peeples ME.** 2000. Glycosaminoglycan sulfation requirements for respiratory syncytial virus infection. J. Virol. **74**:10508–10513.
19. **Holt PG, Strickland DH, Wikstrom ME, Jahnsen FL.** 2008. Regulation of immunological homeostasis in the respiratory tract. Nat. Rev. Immunol. **8**:142–152.
20. **Huang Q, et al.** 2001. The plasticity of dendritic cell responses to pathogens and their components. Science **294**:870–875.
21. **Humlicek AL, et al.** 2007. Paracellular permeability restricts airway epithelial responses to selectively allow activation by mediators at the basolateral surface. J. Immunol. **178**:6395–6403.
22. **Hussell T, Goulding J.** 2010. Structured regulation of inflammation during respiratory viral infection. Lancet Infect. Dis. **10**:360–366.
23. **Jenner RG, Young RA.** 2005. Insights into host responses against pathogens from transcriptional profiling. Nat. Rev. Microbiol. **3**:281–294.
24. **Jewell NA, et al.** 2010. Lambda interferon is the predominant interferon induced by influenza A virus infection in vivo. J. Virol. **84**:11515–11522.
25. **Jewell NA, et al.** 2007. Differential type I interferon induction by respiratory syncytial virus and influenza a virus in vivo. J. Virol. **81**:9790–9800.
26. **Kato A, Schleimer RP.** 2007. Beyond inflammation: airway epithelial cells are at the interface of innate and adaptive immunity. Curr. Opin. Immunol. **19**:711–720.
27. **Kular RK, et al.** 2009. GAGE, an antiapoptotic protein binds and modulates the expression of nucleophosmin/B23 and interferon regulatory factor 1. J. Interferon Cytokine Res. **29**:645–655.
28. **Labrada L, Liang XH, Zheng W, Johnston C, Levine B.** 2002. Age-dependent resistance to lethal alphavirus encephalitis in mice: analysis of gene expression in the central nervous system and identification of a novel interferon-inducible protective gene, mouse ISG12. J. Virol. **76**:11688–11703.
29. **Liu P, et al.** 2007. Retinoic acid-inducible gene I mediates early antiviral response and Toll-like receptor 3 expression in respiratory syncytial virus-infected airway epithelial cells. J. Virol. **81**:1401–1411.
30. **Lopez-Souza N, et al.** 2004. Resistance of differentiated human airway epithelium to infection by rhinovirus. Am. J. Physiol. **286**:L373–L381.
31. **Martinez I, Lombardia L, Garcia-Barreno B, Dominguez O, Melero JA.** 2007. Distinct gene subsets are induced at different time points after human respiratory syncytial virus infection of A549 cells. J. Gen. Virol. **88**:570–581.
32. **Mizgerd JP.** 2008. Acute lower respiratory tract infection. N. Engl. J. Med. **358**:716–727.
33. **Mordstein M, et al.** 2008. Interferon-lambda contributes to innate immunity of mice against influenza A virus but not against hepatotropic viruses. PLoS Pathog. **4**:e1000151.
34. **Openshaw PJ.** 2005. Antiviral immune responses and lung inflammation after respiratory syncytial virus infection. Proc. Am. Thorac Soc. **2**:121–125.
35. **Pankla R, et al.** 2009. Genomic transcriptional profiling identifies a candidate blood biomarker signature for the diagnosis of septicemic melioidosis. Genome Biol. **10**:R127.
36. **Papi A, Luppi F, Franco F, Fabbri LM.** 2006. Pathophysiology of exacerbations of chronic obstructive pulmonary disease. Proc. Am. Thorac. Soc. **3**:245–251.
37. **Peebles RS, Jr, Graham BS.** 2005. Pathogenesis of respiratory syncytial virus infection in the murine model. Proc. Am. Thorac. Soc. **2**:110–115.
38. **Pickles RJ, et al.** 1998. Limited entry of adenovirus vectors into well-differentiated airway epithelium is responsible for inefficient gene transfer. J. Virol. **72**:6014–6023.
39. **Pinto RA, Arredondo SM, Bono MR, Gaggero AA, Diaz PV.** 2006. T helper 1/T helper 2 cytokine imbalance in respiratory syncytial virus infection is associated with increased endogenous plasma cortisol. Pediatrics **117**:e878–e886.
40. **Qureshi F, Pestian J, Davis P, Zaritsky A.** 1998. Effect of nebulized

ipratropium on the hospitalization rates of children with asthma. N. Engl. J. Med. **339**:1030–1035.
41. **Ramilo O, et al.** 2007. Gene expression patterns in blood leukocytes discriminate patients with acute infections. Blood **109**:2066–2077.
42. **Rosebeck S, Leaman DW.** 2008. Mitochondrial localization and pro-apoptotic effects of the interferon-inducible protein ISG12a. Apoptosis **13**:562–572.
43. **Rowe RK, Brody SL, Pekosz A.** 2004. Differentiated cultures of primary hamster tracheal airway epithelial cells. In vitro Cell. Dev. Biol. Anim. **40**:303–311.
44. **Schleimer RP, Kato A, Kern R, Kuperman D, Avila PC.** 2007. Epithelium: at the interface of innate and adaptive immune responses. J. Allergy Clin. Immunol. **120**:1279–1284.
45. **Schmid S, Mordstein M, Kochs G, Garcia-Sastre A, Tenoever BR.** 2010. Transcription factor redundancy ensures induction of the antiviral state. J. Biol. Chem. **285**:42013–42022.
46. **Shapira SD, et al.** 2009. A physical and regulatory map of host-influenza interactions reveals pathways in H1N1 infection. Cell **139**:1255–1267.
47. **Shaykhiev R, Bals R.** 2007. Interactions between epithelial cells and leukocytes in immunity and tissue homeostasis. J. Leukoc. Biol. **82**:1–15.
48. **Shornick LP, et al.** 2008. Airway epithelial versus immune cell Stat1 function for innate defense against respiratory viral infection. J. Immunol. **180**:3319–3328.
49. **Spann KM, Tran KC, Chi B, Rabin RL, Collins PL.** 2004. Suppression of the induction of alpha, beta, and lambda interferons by the NS1 and NS2 proteins of human respiratory syncytial virus in human epithelial cells and macrophages. J. Virol. **78**:4363–4369.
50. **Taubenberger JK, Morens DM.** 2008. The pathology of influenza virus infections. Annu. Rev. Pathol. **3**:499–522.
51. **Thompson CI, Barclay WS, Zambon MC, Pickles RJ.** 2006. Infection of human airway epithelium by human and avian strains of influenza A virus. J. Virol. **80**:8060–8068.
52. **Ueno K, et al.** 2008. MUC1 mucin is a negative regulator of Toll-like receptor signaling. Am. J. Respir. Cell Mol. Biol. **38**:263–268.
53. **Varga ZT, et al.** 2011. The influenza virus protein PB1-F2 inhibits the induction of type I interferon at the level of the MAVS adaptor protein. PLoS Pathog. **7**:e1002067.
54. **Wang J, et al.** 2009. Differentiated human alveolar type II cells secrete antiviral IL-29 (IFN-lambda 1) in response to influenza A infection. J. Immunol. **182**:1296–1304.
55. **Weslow-Schmidt JL, et al.** 2007. Type I interferon inhibition and dendritic cell activation during gammaherpesvirus respiratory infection. J. Virol. **81**:9778–9789.
56. **Yoboua F, Martel A, Duval A, Mukawera E, Grandvaux N.** 2010. Respiratory syncytial virus-mediated NF-kappa B p65 phosphorylation at serine 536 is dependent on RIG-I, TRAF6, and IKK beta. J. Virol. **84**:7267–7277.
57. **You Y, Richer EJ, Huang T, Brody SL.** 2002. Growth and differentiation of mouse tracheal epithelial cells: selection of a proliferative population. Am. J. Physiol. **283**:L1315–L1321.
58. **Zaas AK, et al.** 2009. Gene expression signatures diagnose influenza and other symptomatic respiratory viral infections in humans. Cell Host Microbe **6**:207–217.
59. **Zhang L, et al.** 2005. Infection of ciliated cells by human parainfluenza virus type 3 in an in vitro model of human airway epithelium. J. Virol. **79**:1113–1124.
60. **Zhang L, Peeples ME, Boucher RC, Collins PL, Pickles RJ.** 2002. Respiratory syncytial virus infection of human airway epithelial cells is polarized, specific to ciliated cells, and without obvious cytopathology. J. Virol. **76**:5654–5666.